

Nanobody Paratope Mapping using Native Mass Spectrometry and Ultraviolet Photodissociation

Luis A. Macias,^a Xun Wang,^b Bryan W. Davies,^b Jennifer S. Brodbelt^{a*}

^aDepartment of Chemistry, University of Texas at Austin, Austin, TX 78712, USA

^bDepartment of Molecular Biosciences, University of Texas at Austin, Austin, TX 78712, USA

Correspondence: jbroadbelt@cm.utexas.edu

Supporting Information

Table of Contents

	Content	Page no.
1	Figure S1. Native MS1 spectra of free proteins	S2
2	Figure S2. UVPD mass spectra of free nanobodies	S3
3	Figure S3. Free and bound nanobody fragment maps	S4
4	Figure S4. Gnb UVPD fragment heatmap	S5
5	Figure S5. Rnb UVPD fragment heatmap	S6
6	Figure S6. Anb UVPD fragment heatmap	S7
7	Figure S7. nb structure mapped with UVPD enhancement	S8
	Figure S8. CDR regions mapped onto crystal structures of (A) Gnb, (B) Rnb, and (C) Anb	S9
8	Figure S9. Charge site analysis of RNnb	S10
9	Figure S10. Charge site analysis of Anb	S11

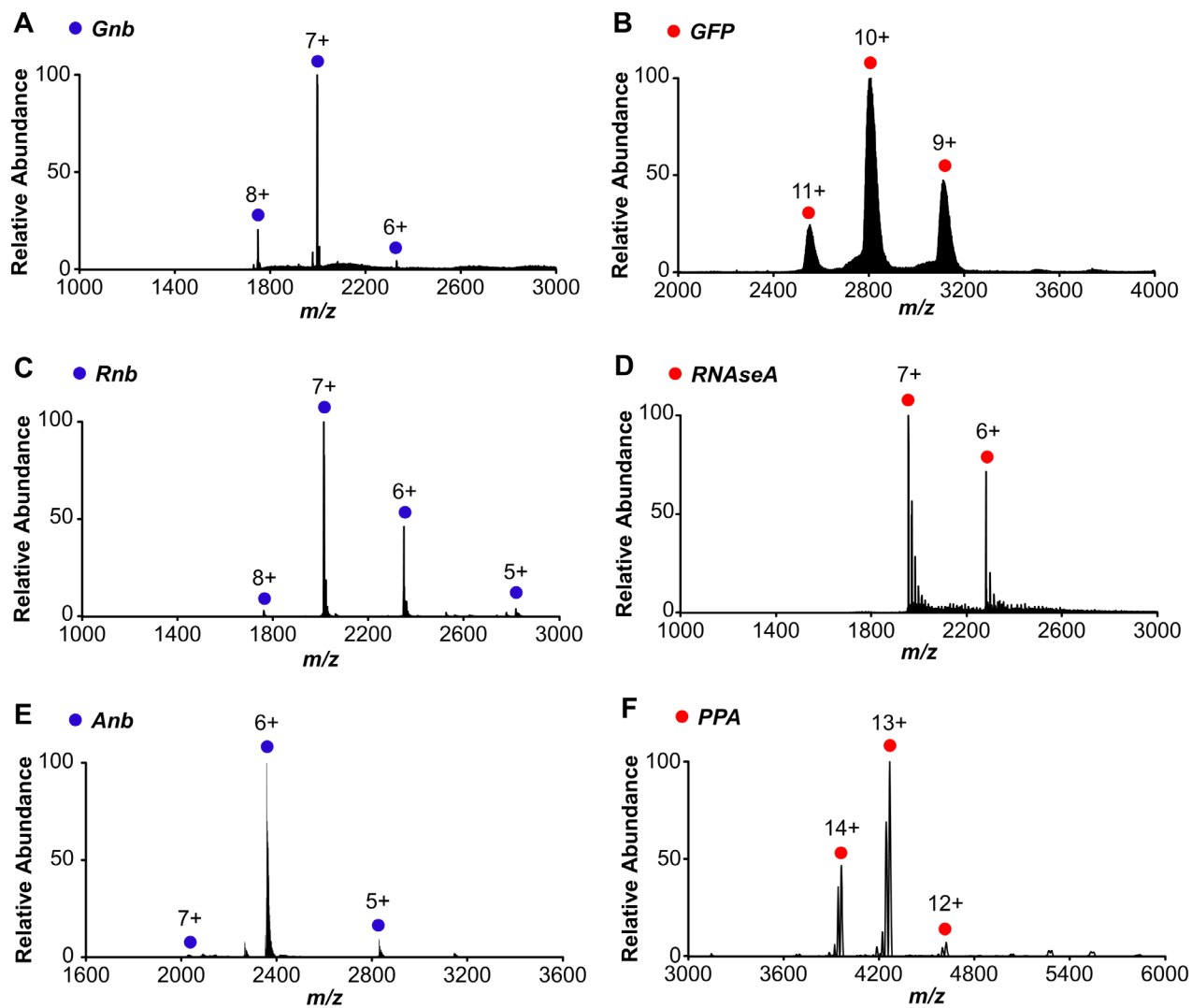


Figure S1. Native MS1 mass spectra of apo nanobodies and the apo antigens. (A) free Gnb and (B) free GFP; (C) free Rnb and (D) free RNaseA; (E) free Anb and (B) free PPA. Each solution contained 30 μ M protein in 100 mM ammonium acetate.

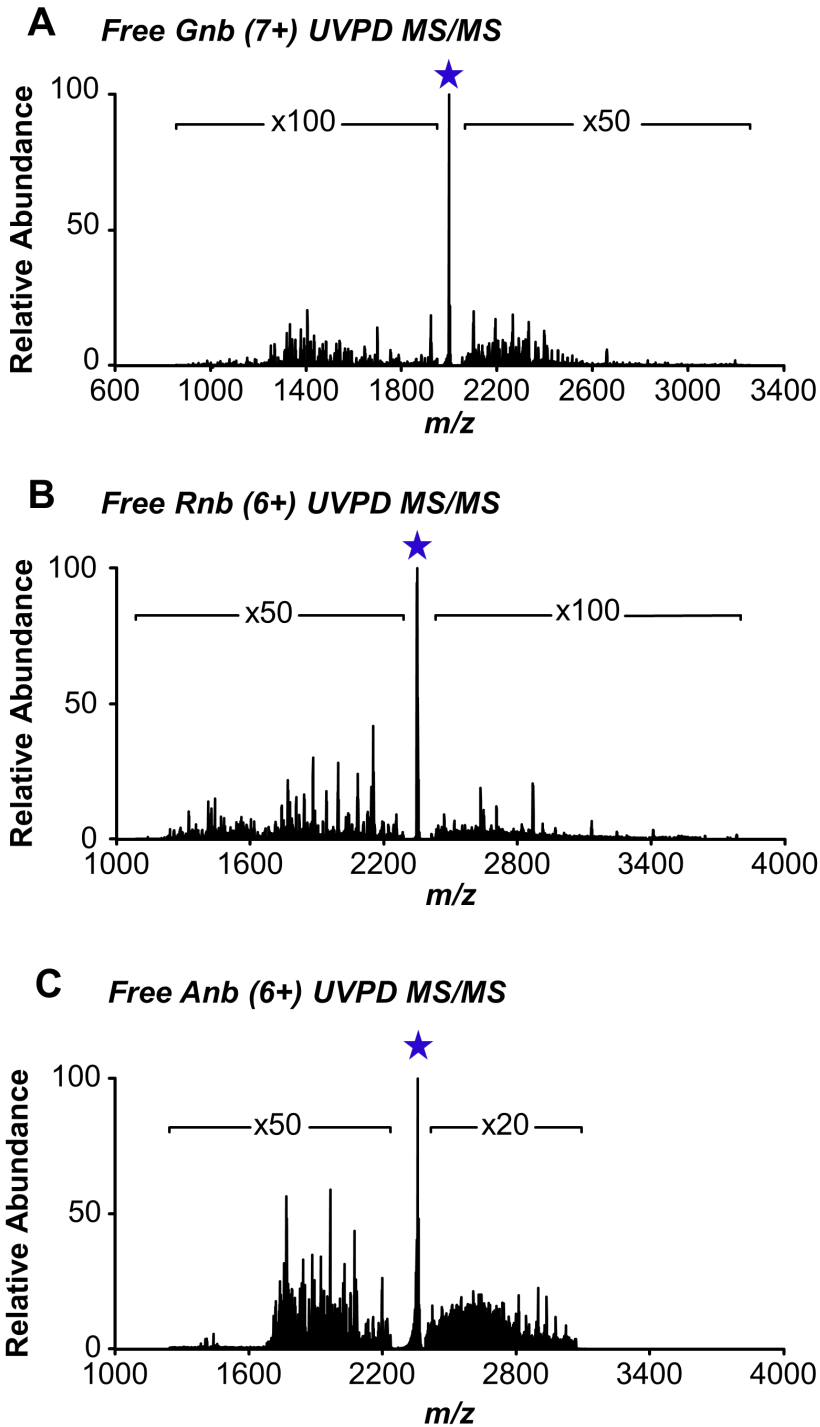


Figure S2. UVPD (1 pulse set to 3 mJ) mass spectra of each of the three nanobodies. (A) free Gnb (7+), (B) free Rnb (6+), and (C) free Anb (6+). Regions of interest with low abundance sequence fragments are magnified. Precursor ions are demarcated with a star.

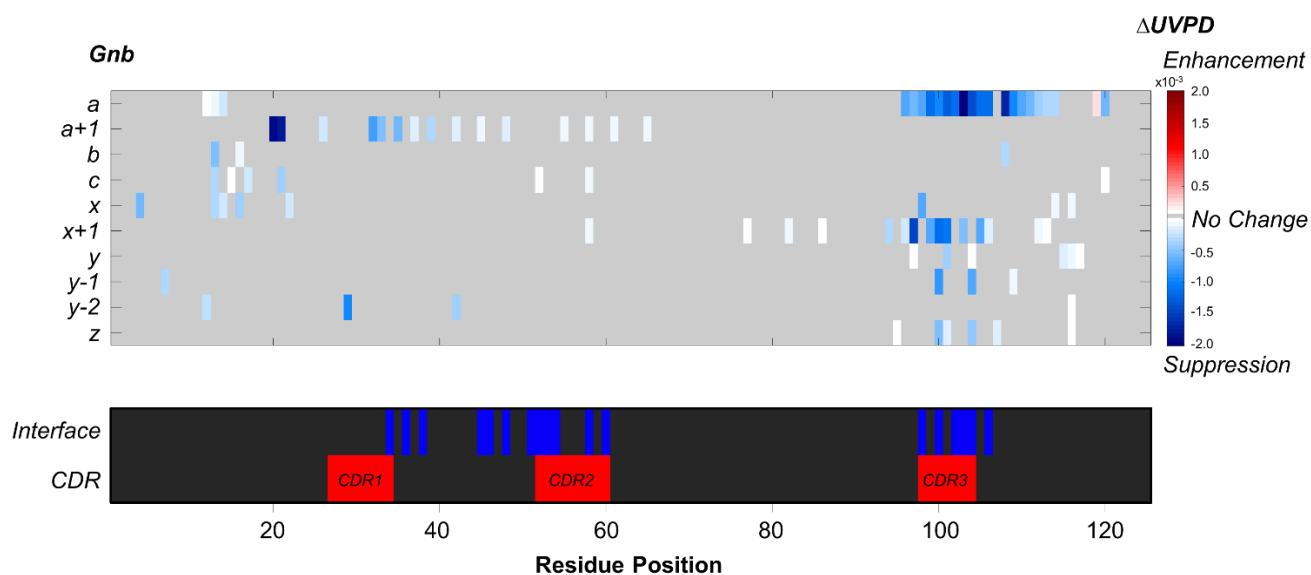


Figure S4. Suppression and enhancement of backbone cleavage sites based on abundances of UVPD fragment ions induced for Gnb by antigen binding. Heat plots display significant differences ($p < 0.05$, $n = 5$) for the abundances of each UVPD fragment type between the free and bound states. Blue and red indicate suppression and enhancement of fragment abundances, respectively, for the nanobody upon complexation. Positions that display no significant change are shown in grey. Color maps highlighting interface residues and CDRs are also included. $\Delta UVPD$ values correspond to the fragment abundance per residue for the bound state minus the fragment abundance per residue for the free state.

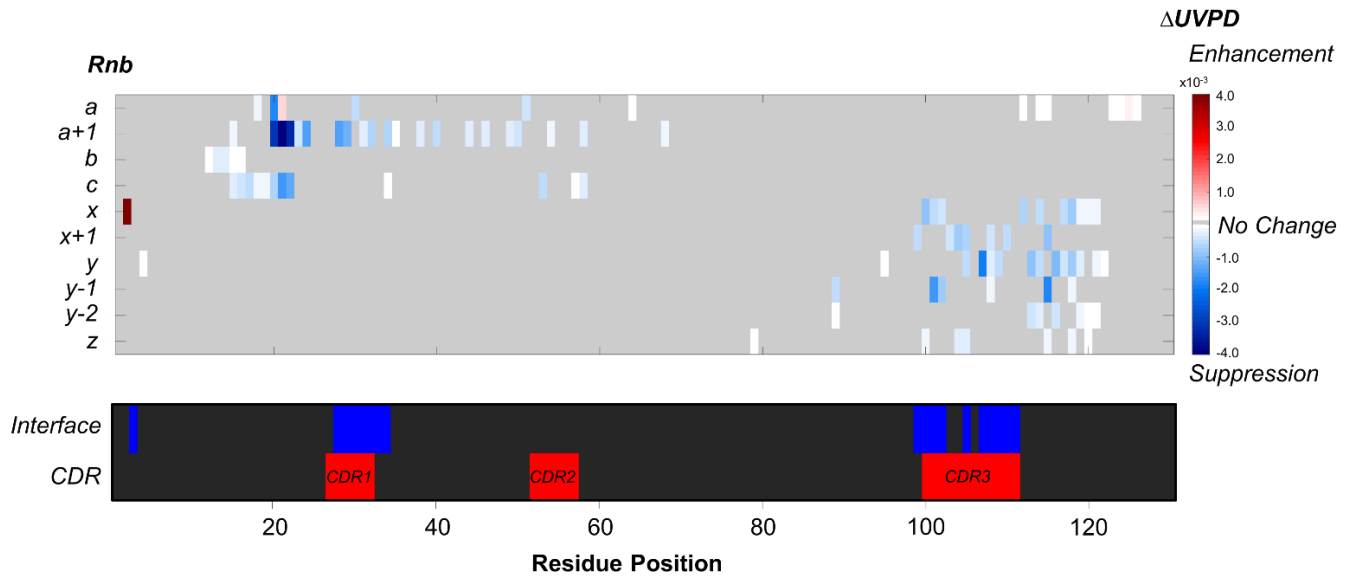


Figure S5. Suppression and enhancement of backbone cleavage sites based on abundances of UVPD fragment ions induced for Rnb by antigen binding. Heat plots display significant differences ($p < 0.05$, $n = 5$) for the abundances of each UVPD fragment type between the free and bound states. Blue and red indicate suppression and enhancement of fragment abundances, respectively, for the nanobody upon complexation. Positions that display no significant change are shown in grey. Color maps highlighting interface residues and CDRs are also included. $\Delta UVPD$ values correspond to the fragment abundance per residue for the bound state minus the fragment abundance per residue for the free state.

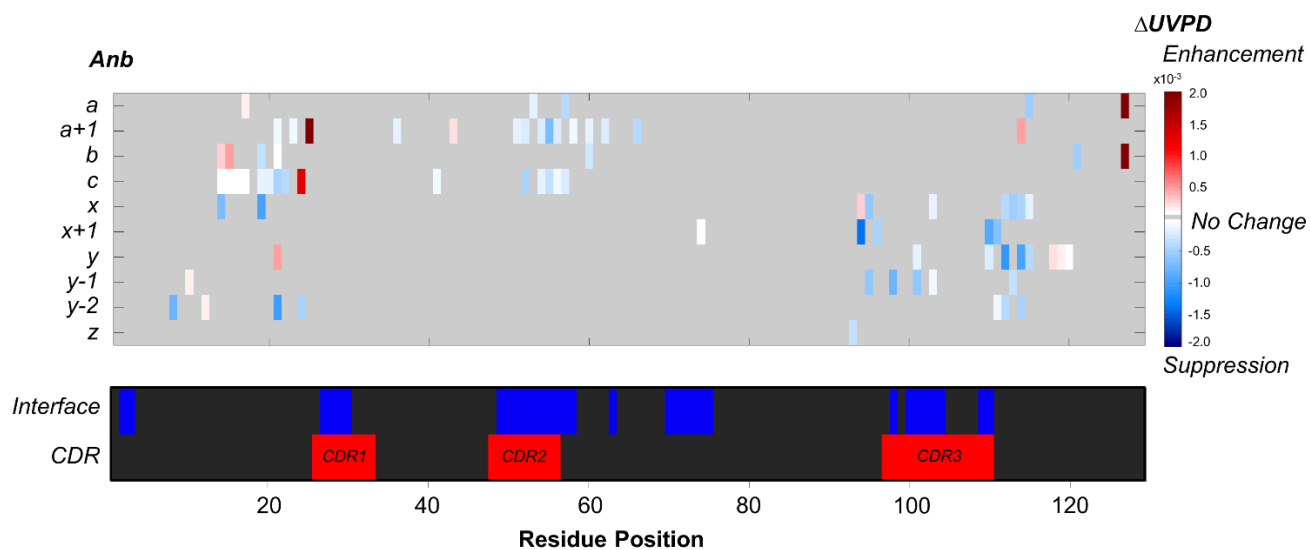


Figure S6. Suppression and enhancement of backbone cleavage sites based on abundances of UVPD fragment ions induced for Anb by antigen binding. Heat plots display significant differences ($p < 0.05$, $n = 5$) for the abundances of each UVPD fragment type between the free and bound states. Blue and red indicate suppression and enhancement of fragment abundances, respectively, for the nanobody upon complexation. Positions that display no significant change are shown in grey. Color maps highlighting interface residues and CDRs are also included. $\Delta UVPD$ values correspond to the fragment abundance per residue for the bound state minus the fragment abundance per residue for the free state.

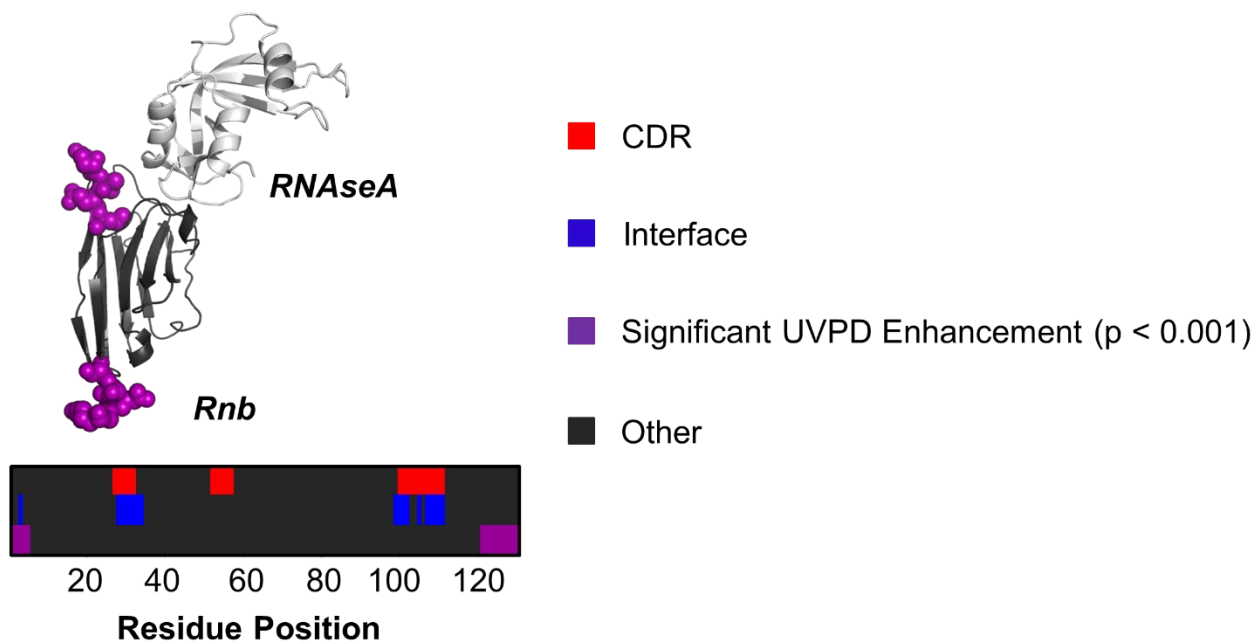


Figure S7. Sections displaying significant UVPD enhancement upon complexation ($p < 0.001$, $n = 0.05$) are mapped onto the crystal structure of Rnb•RNaseA as purple spheres. Residue positions displaying significant UVPD enhancement, interface residues, and CDR regions are shown as color maps.

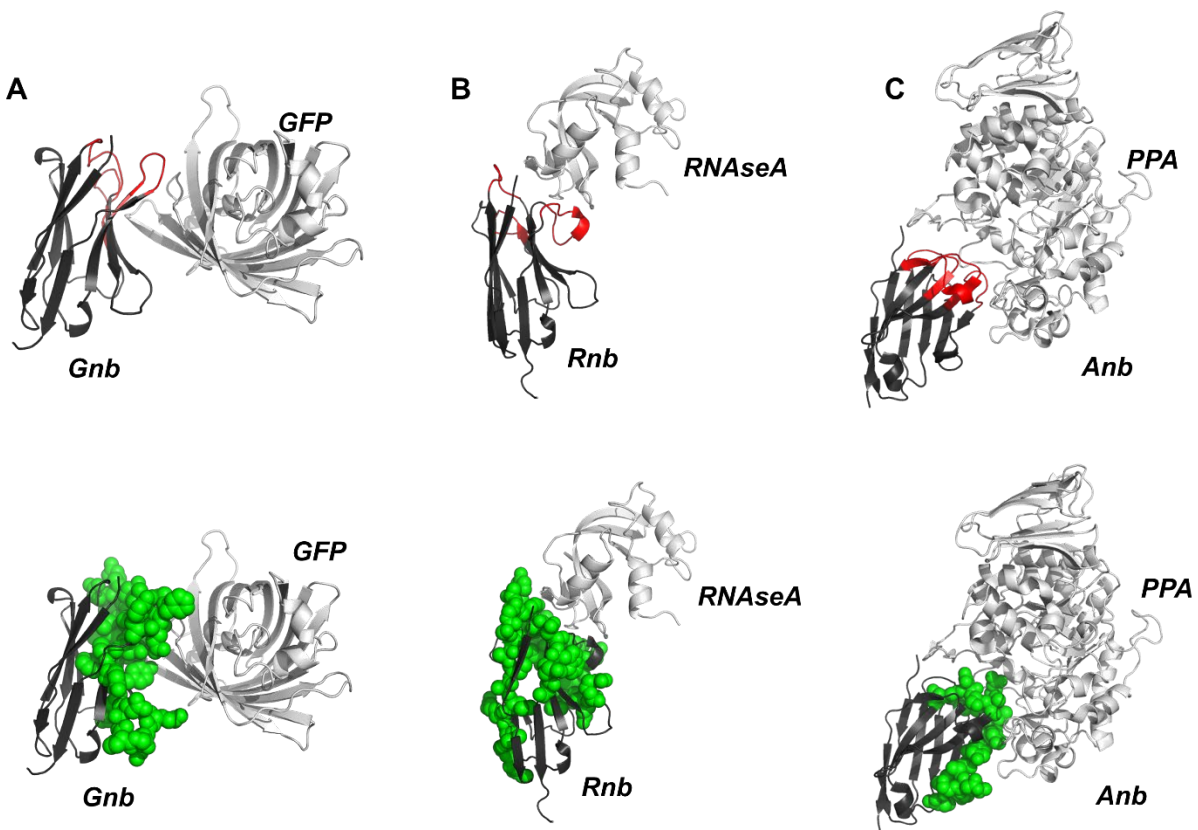


Figure S8. CDR regions in red are mapped onto crystal structures of (A) Gnb, (B) Rnb, and (C) Anb. The UVPD backbone cleavage maps from Figure 3 are shown in the lower portion of the figure to facilitate comparisons.

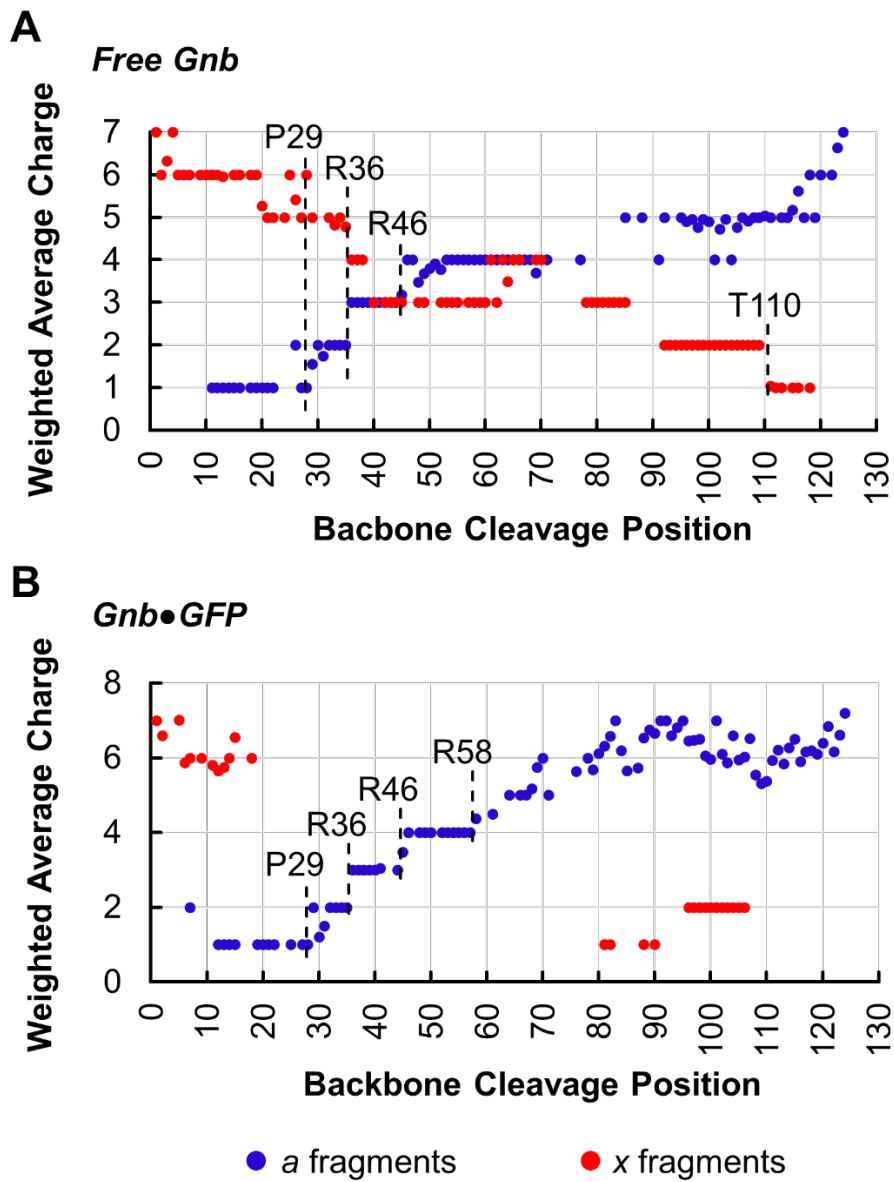


Figure S9. Weighted average charge of *a*-type and *x*-type fragment ions attributed to GFnb produced by UVPD of (A) free GFnb (7+) and (B) GFnb•GFP (13+) delineated based on the backbone cleavage site along the sequence of the nanobody.

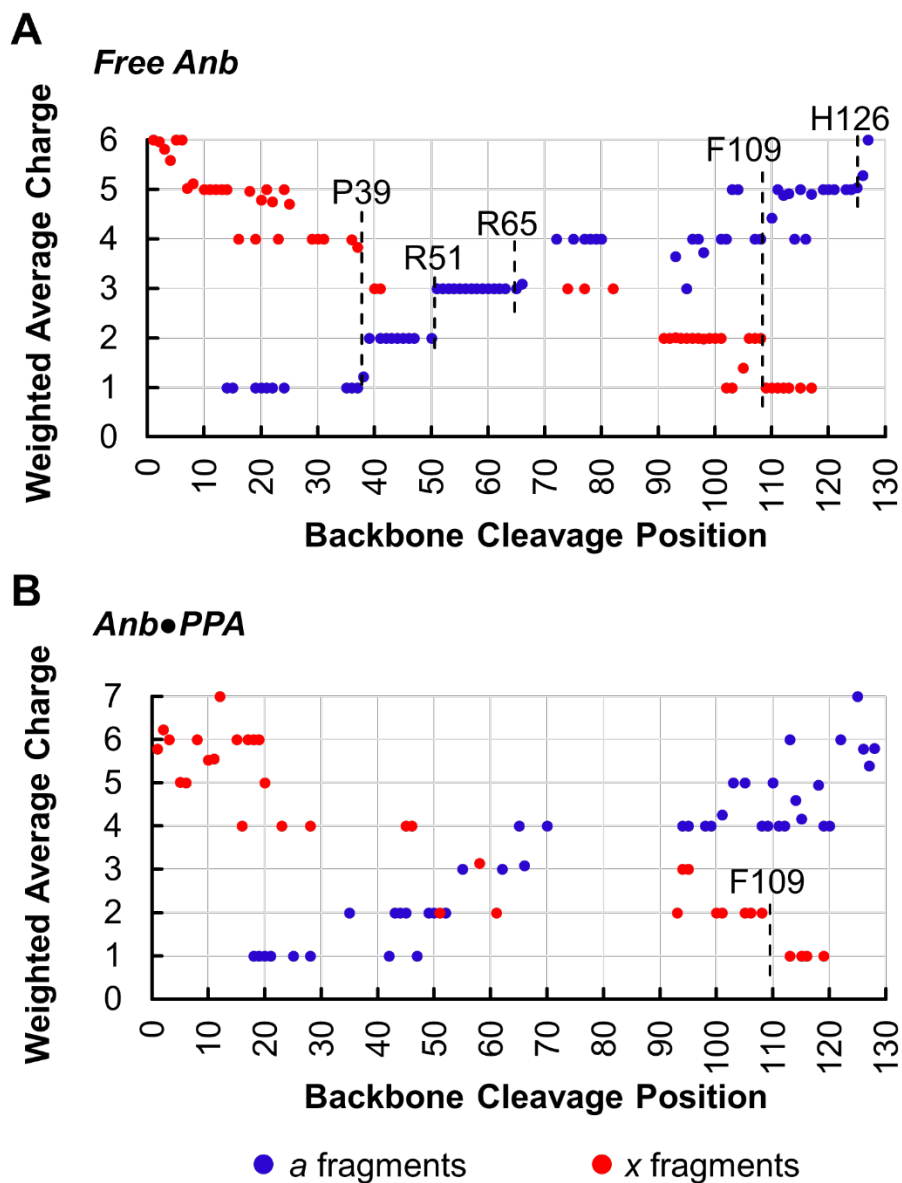


Figure S10. Weighted average charge of *a*-type and *x*-type fragment ions attributed to Anb produced by UVPD of (A) free Anb (6+) and (B) Anb•PPA (15+), delineated based on the backbone cleavage site along the sequence of the nanobody.